

SUPPORTING MATERIAL

***N*-Terminal Alkylation Significantly Improves Biomimicry of a Peptoid Analogue of Surfactant Protein C**

Nathan J. Brown, Michelle T. Dohm, Jorge Bernardino de la Serna, and Annelise E. Barron

Langmuir-Willhelmy surface balance data for AFM imaging – (data taken at 22-23 °C)

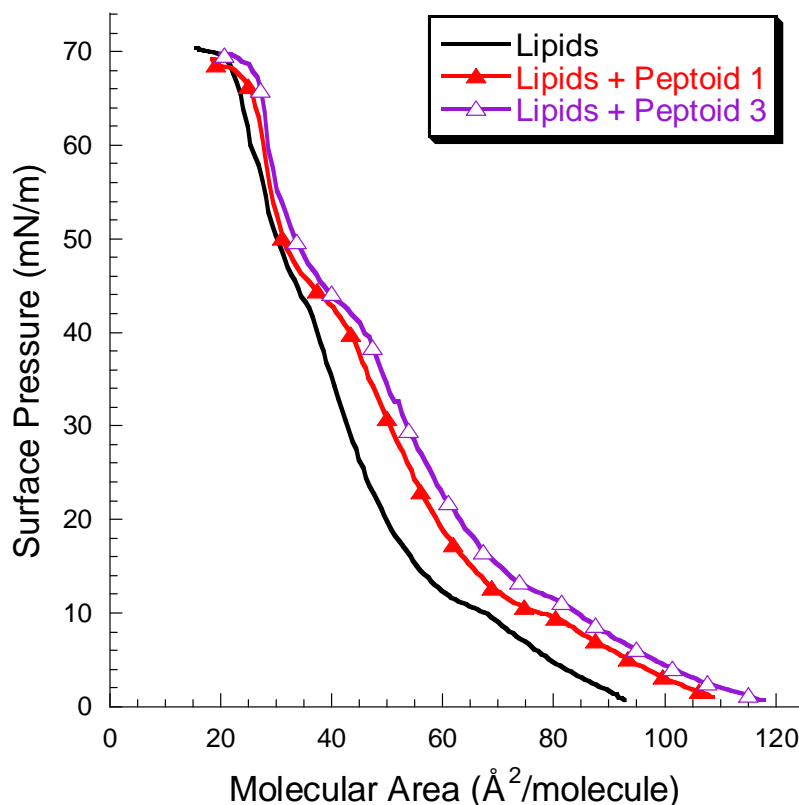


FIGURE S1. LWSB data for AFM imaging at 22-23 °C. First-compression surface pressure (Π)-molecular area (A) LWSB isotherms for three different surfactant formulations. Isotherms were collected on a buffered subphase (150 mM NaCl, 5 mM Tris, pH 7.0) with a unidirectional barrier speed of $50 \text{ cm}^2 \text{ min}^{-1}$. LWSB molecular areas include all surfactant species (lipid plus peptoid SP mimics).

Circular dichroism spectroscopy

Method. Circular dichroism (CD) measurements were performed on a Jasco model 715 spectropolarimeter (Easton, MD) with $\sim 60 \mu\text{M}$ peptoid in methanol. CD spectra were then acquired in a quartz cylindrical cell (Hellma model 121-QS, Forest Hills, NY) with a path length of 0.02 cm, employing a scan rate of 100 nm/min. CD spectra reported here represented the average of 40 successive spectral accumulations. Data were expressed in terms of per-residue molar ellipticity ($\text{deg cm}^2/\text{dmol}$), as calculated per mole of amide groups present and normalized by the molar concentration of peptoid.

Secondary structure. CD was used to characterize and compare the secondary structure in free solution of the peptoid-based SP-C mimics shown in Table 1. The highly helical nature of SP-C has been shown to be essential for its surfactant activity (1-2). CD spectra of the peptoid-based SP-C mimics are displayed in Fig. S2. The non-alkylated and alkylated peptoid-based SP-C mimics containing α -chiral, aromatic residues exhibited CD spectral features that are similar to a peptide α -helix, with each showing an intense maximum at $\lambda \sim 192 \text{ nm}$ and double minima at $\lambda \sim 205 \text{ nm}$ and $\sim 220 \text{ nm}$ (Fig. S2). These spectral features are characteristic signatures of a helical peptoid structure in oligomers of this class, which have highly ordered backbone amide bonds that adopt right-handed conformations with a periodicity of ~ 3 residues per turn and a pitch of $\sim 6 \text{ \AA}$ (3-4).

The intensities of the helical spectrum for the aromatic-based mimics are very similar, with the alkylated mimics, Peptoids 2 and 3, having slightly stronger intensities than the non-alkylated mimic, Peptoid 1. Regardless of the degree of alkylation, all of the SP-C mimics are shown to be helical and structured in solution, satisfying one of the structural criteria, helicity, believed to be of importance for the surface activity of SP-C (2).

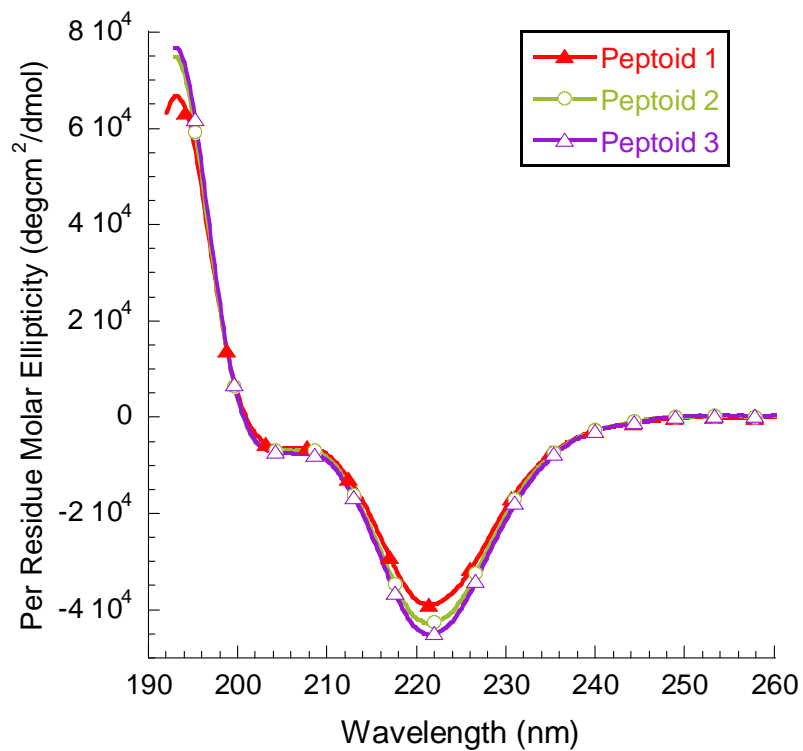


FIGURE S2 Circular dichroism (CD) spectra of peptoid-based SP-C mimics (Peptoid 1, Peptoid 2, and Peptoid 3), showing qualitatively similar secondary structure characteristics of peptoid helices. Spectra were acquired in methanol at a concentration of $\sim 60 \mu\text{M}$ in methanol at room temperature.

Static-bubble pulsating bubble surfactometry

Static-surfactant adsorption. One of the essential biophysical properties of native LS is its unique ability to rapidly adsorb from the alveolar subphase to the air-liquid interface, forming a surface-active layer that regulates surface tension during the respiration cycle (5-6). On their own, the phospholipids of LS exhibit poor adsorption kinetics and spreading properties; however, the addition of the hydrophobic surfactant proteins to the phospholipids dramatically improves these characteristics, reaching an equilibrium surface tension of ~ 25 mN/m in less than a minute (7-11). A modified PBS run in static mode was used to characterize the adsorption kinetics of the lipid mixture alone and with the addition of 1.6 mol% SP-C protein and SP-C mimics. Fig. S3 displays the static surface tension as a function of time for the various surfactant formulations.

In the absence of SP-C protein or SP-C mimetics, the lipid mixture displays very slow surface adsorption and fails to reach an equilibrium surface tension lower than 51 mN/m even after 20 minutes (Fig. S3). The addition of the SP-C protein to the lipid formulation significantly accelerated the kinetics of surfactant adsorption to the interface. The SP-C protein allowed the film to reach a surface tension of approximately 26 mN/m in less than one minute and a final equilibrium surface tension of ~ 24 mN/m. The addition of the non-alkylated peptoid, Peptoid 1, to the lipid formulation also results in accelerated adsorption kinetics over the lipids alone, although, the rate is slower than the formulation containing SP-C, reaching a static adsorptive surface tension of ~ 37 mN/m after 1 minute and a final equilibrium surface tension of ~ 31 mN/m. Introducing one or two alkyl chains in the *N*-terminal region of the peptoid does not significantly alter the film adsorption kinetics. Both the formulations containing either Peptoid 2 or Peptoid 3 exhibit much improved adsorption kinetics over the lipid formulation alone, although, not quite to the extent that the native protein does so.

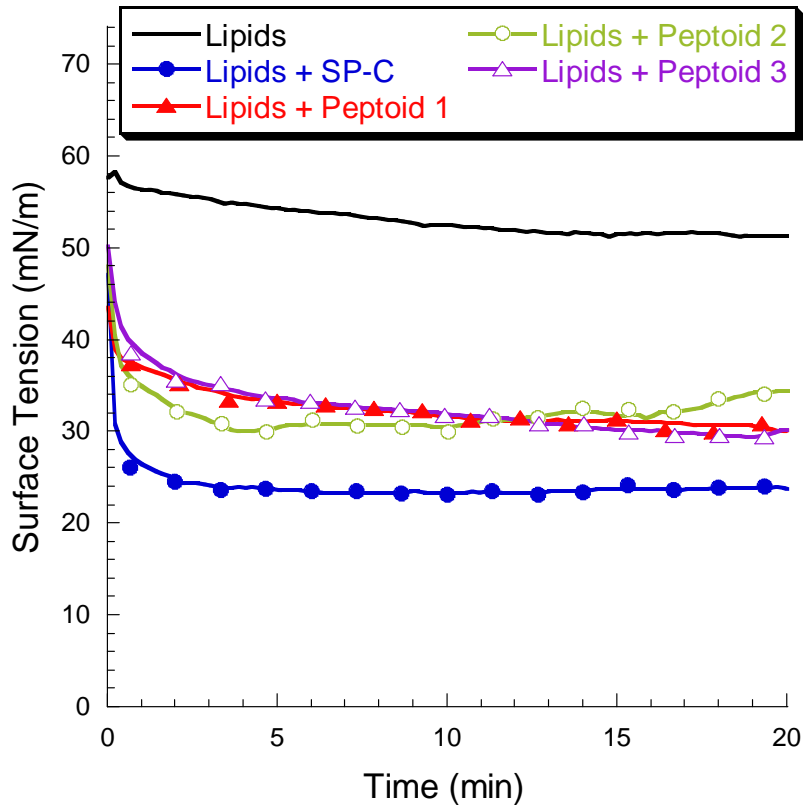


FIGURE S3 Static pulsating bubble surfactometry (PBS) results displaying surface tension as a function of time. Measurements were taken at a bulk lipid concentration of 1 mg/mL lipids at 37°C. LWSB molecular areas include all surfactant species, lipid plus SP-C/peptoid.

TABLE S1 Static PBS adsorption at selected time intervals. Measurements were taken at a bulk lipid concentration of 1 mg/mL at 37°C.

Formulation	1 min	2.5 min	5 min	10 min	20 min
	γ_{ads}	γ_{ads}	γ_{ads}	γ_{ads}	γ_{ads}
Lipids	54.3 ± 3.4	53.7 ± 3.2	52.8 ± 2.9	51.4 ± 2.8	51.1 ± 2.7
Lipids + SP-C	26.4 ± 1.8	25.5 ± 2.2	24.7 ± 1.8	24.8 ± 2.4	24.6 ± 2.2
Lipids + Peptoid 1	37.7 ± 2.1	36.1 ± 2.6	32.8 ± 2.3	32.7 ± 1.5	31.5 ± 2.0
Lipids + Peptoid 2	33.1 ± 3.3	32.3 ± 2.7	31.4 ± 0.52	29.7 ± 0.73	30.7 ± 3.3
Lipids + Peptoid 3	37.1 ± 2.8	35.1 ± 3.0	33.0 ± 2.9	31.2 ± 1.9	31.2 ± 2.4

Data are mean $\gamma \pm$ SD in mN/m.

Langmuir-Willhelmy surface balance – 25°C

TABLE S2 LWSB compression and re-spreading at 25°C.

Formulation	1 st Compression		3 rd Compression		% Recovery*	
	Liftoff Area	Area at 30 mN/m	Liftoff Area	Area at 30 mN/m	Liftoff	30 mN/m
Lipids	91.4 ± 3.0	42.8 ± 0.5	70.4 ± 3.6	35.2 ± 1.7	77.0 ± 3.9	82.2 ± 3.5
Lipids + SP-C	95.9 ± 3.0	43.7 ± 1.8	78.7 ± 1.8	38.2 ± 1.1	82.1 ± 2.0	88.0 ± 2.1
Lipids + Peptoid 1	101.1 ± 2.4	47.1 ± 0.8	83.9 ± 1.9	41.9 ± 1.0	83.1 ± 2.9	89.0 ± 2.5
Lipids + Peptoid 2	104.5 ± 4.2	48.3 ± 0.9	87.7 ± 2.9	44.0 ± 1.6	83.9 ± 3.3	91.1 ± 2.6
Lipids + Peptoid 3	104.7 ± 2.3	47.9 ± 1.0	88.4 ± 2.4	45.3 ± 0.9	84.5 ± 3.6	94.7 ± 1.0

Data are mean ± SD in Å²/molecule. * % recovery refers to the percent molecular area at either liftoff or 30 mN/m on the third compression relative to the molecular area of the corresponding feature on the first compression.

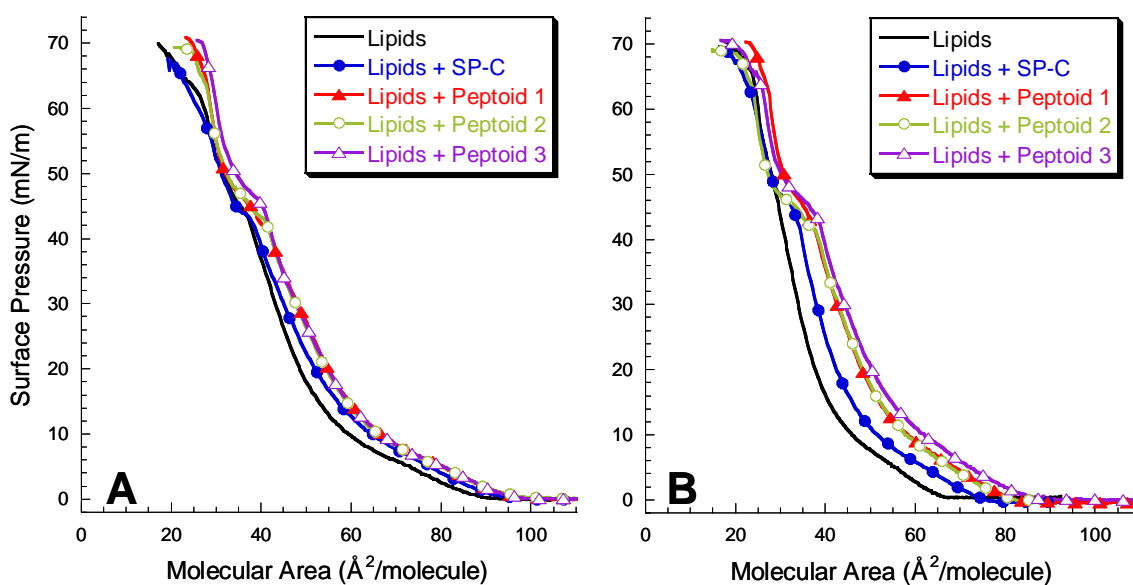


FIGURE S4 LWSB studies at 25°C. (A) First compression surface pressure (Π)-area (A) LWSB isotherms for the surfactant formulations; (B) Third compression Π -A isotherms obtained for the surfactant formulations. Isotherms were collected on a buffered subphase (150 mM NaCl, 10 mM HEPES, 5 mM CaCl₂, pH 6.9) at 25°C. LWSB molecular areas include all surfactant species, lipid plus SP-C/peptoid.

Langmuir-Willhelmy surface balance – 37°C

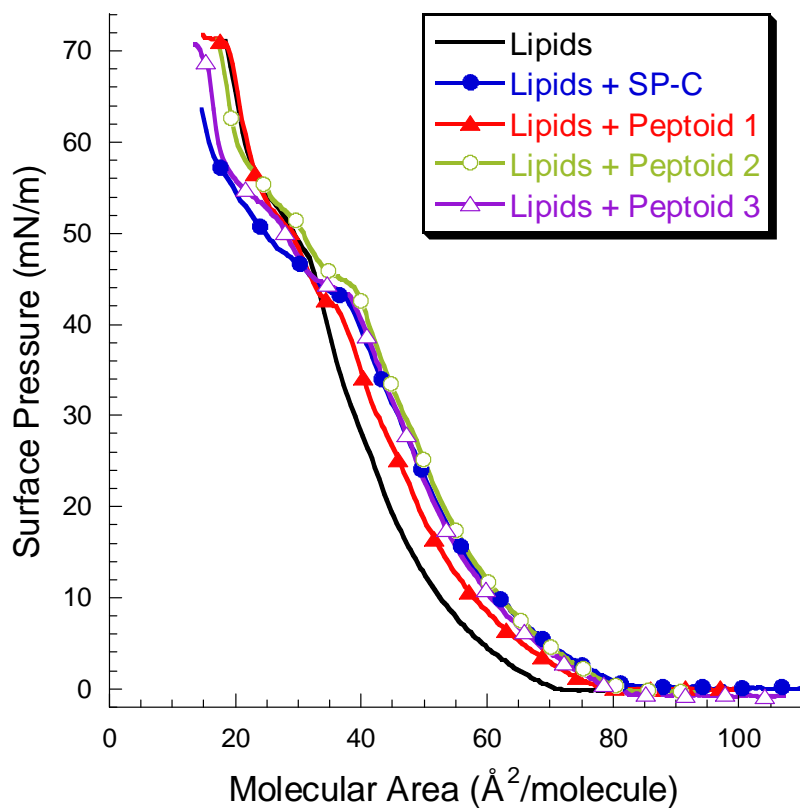


FIGURE S5 LWSB studies at 37°C. Third compression Π -A isotherms obtained for the surfactant formulations collected on a buffered subphase (150 mM NaCl, 10 mM HEPES, 5 mM CaCl₂, pH 6.9) at 37°C. LWSB molecular areas include all surfactant species, lipid plus SP-C/peptoid.

References

1. Johansson, J., G. Nilsson, R. Stromberg, B. Robertson, H. Jornvall, and T. Curstedt. 1995. Secondary structure and biophysical activity of synthetic analogs of the pulmonary surfactant polypeptide SP-C. *Biochem. J* 307:535-541.
2. Clercx, A., G. Vandenbussche, T. Curstedt, J. Johansson, H. Jornvall, and J. F. Ruyschaert. 1995. Structural and functional importance of the C-terminal part of the pulmonary surfactant polypeptide SP-C. *Eur. J. Biochem.* 229:465-472.
3. Armand, P., K. Kirshenbaum, R. A. Goldsmith, S. Farr-Jones, A. E. Barron, K. T. V. Truong, K. A. Dill, D. F. Mierke, F. E. Cohen, R. N. Zuckermann, and E. K. Bradley. 1998. NMR determination of the major solution conformation of a peptoid pentamer with chiral side chains. *Proc. Natl. Acad. Sci. U. S. A.* 95:4309-4314.
4. Wu, C. W., T. J. Sanborn, K. Huang, R. N. Zuckermann, and A. E. Barron. 2001. Peptoid oligomers with alpha-chiral, aromatic side chains: sequence requirements for the formation of stable peptoid helices. *J. Am. Chem. Soc.* 123:6778-6784.
5. Johansson, J., T. Curstedt, and B. Robertson. 2001. Artificial surfactants based on analogues of SP-B and SP-C. *Pediatr. Pathol. Mol. Med.* 20:501-518.
6. Notter, R. H. 2000. Lung surfactants : basic science and clinical applications. Marcel Dekker, New York.
7. Oosterlaken-Dijksterhuis, M. A., H. P. Haagsman, L. M. G. Vangolde, and R. A. Demel. 1991. Characterization of lipid insertion into monomolecular layers mediated by lung surfactant proteins SP-B and SP-C. *Biochemistry* 30:10965-10971.
8. Perez-Gil, J., J. Tucker, G. Simatos, and K. M. W. Keough. 1992. Interfacial adsorption of simple lipid mixtures combined with hydrophobic surfactant protein from pig lung. *Biochem. Cell Biol.* 70:332-338.
9. Wang, Z. D., S. B. Hall, and R. H. Notter. 1996. Roles of different hydrophobic constituents in the adsorption of pulmonary surfactant. *J. Lipid Res.* 37:790-798.
10. Whitsett, J. A., B. L. Ohning, G. Ross, J. Meuth, T. Weaver, B. A. Holm, D. L. Shapiro, and R. H. Notter. 1986. Hydrophobic surfactant-associated protein in whole lung surfactant and its importance for biophysical activity in lung surfactant extracts used for replacement therapy. *Pediatr. Res.* 20:460-467.
11. Yu, S. H., and F. Possmayer. 1990. Role of bovine pulmonary surfactant-associated proteins in the surface-active property of phospholipid mixtures. *Biochim. Biophys. Acta* 1046:233-241.